ISSN 2277 – 5528
Impact Factor- 4.015

INTERNATIONAL JOURNAL OF ENGINEERING SCIENCES &MANAGEMENT

THE EFFECT OF TERNARY ELEMENT FE ON MECHANICAL PROPERTIES IN NITI SHAPE MEMORY ALLOYS

Naresh H[*1], Prashantha.S[2] & Bharath H S[3]
[*1]Christ University, Bengaluru-560074, India
[2&3]Siddaganga Institute of Technology, BH, Road Tumkur- 572103, India

ABSTRACT

The influences of Fe-addition on phase transformation behavior, mechanical properties and microstructure of $Ti_{50}Ni_{50-x}Fe_x$ alloys were investigated by means of optical microscopy, Differential Scanning Calorimetry and X-ray diffraction (XRD). Results indicate that, as a substitute for Ni, Fe added to TiNi alloys can dramatically decrease the martensite transformation temperature and R phase transformation and martensite transformation are accordingly separated. The results show that TiNiFe alloys exhibit two-step martensitic transformation. The start temperature of martensitic transformation increases sharply from 245 K to 267 K when 4 % Fe is added in, and then decreases gradually if Fe content further increases. The hardness of TiNiFe ternary alloys before heat treatment is constant for up to 4% of the composition and suddenly increases for 8% composition and also it behaves same for heat treated specimens because of formation of equilibrium precipitates Ni_3Ti formation.

Keywords*: TiNiFe; Shape Memory Alloy; Martensite Transformation; Mechanical Properties; Microstructure.*

I. INTRODUCTION

Near-equiatomic NiTi shape memory alloys (SMAs) have found wide application in aerospace, aviation, and medical industries owing to their superior functional properties of shape memory effect (super elasticity), biocompatibility as well as excellent mechanical properties [1-16]. In order to modify and ameliorate the properties of the NiTi alloys to meet specific requirements by unique users, addition of tiny amounts of some alloying elements into the binary and ternary SMAs has become a well-known adopted means and way.

However, different alloying elements will exert different influences upon the alloys having the identical basic composition. For example, in the ternary alloys Ni-Ti-*X*, if *X* is referred to Pd, Hf, Pt, or Zr, they exhibit relatively high martensitic start transformation temperature (M_S)[17-27], and if *X* is referred to Fe, Nb, Mo, Al, they have a sharply decreased M_S [28-31] Recently, much more efforts have been devoted, experimentally or theoretically, to the study on the effects of adding ternary element on NiTi-, Cu-, and Fe-based SMAs [transformation temperature of TiNi-based alloys varies dramatically with their composition. A slight and adding the third element can also influence the mechanical properties of the NiTi- based alloys[21-31] Till now, a lot of studies have been devoted to the influences of the third element like Fe, Cu, Nb, etc., on the transformation behaviour and shape memory effects and/or super elasticity[21-27,31-36]. In 1971, elastic properties of TiNiFe shape memory alloy wires were evaluated by Andresen to develop TiNi-based TiNi-based shape memory alloys for medical application [10]. However, phase transformation behaviour and mechanical properties of TiNiFe alloy have not been reported. The present paper is aimed to fill this void. The present work is carried out on the basic Ti-Ni-Fe ternary alloys. These alloys, as distinct from NiTi binary alloys, generally show a two-step phase transformation on both cooling and heating processes without any special thermal and thermo mechanical treatments. This makes it easy to study the influences of adding RE on the two-phase transformation. In order to facilitate revealing the effects of RE on the phase transformation and microstructure of Ti_{50} $Ni_{48}Fe_2$ SMAs.

ISSN 2277 – 5528
Impact Factor- 4.015

Nomenclature

Ni	Nickel
Ti	Titanium
Fe	Iron
Cu	Copper
Pd	Palladium
Hf	Hafnium
Pt	Platinum
Zr	Zirconium

II. METHODOLOGY & MATERIAL

Preparation of samples by melting Nitinol with the addition of Ternary alloying additions (Fe) to the nearly equiatomic NiTi alloys shown in table 3.1 ,their atomic mass % shown in table 3.2 and casting into ingots (rods) The rod to be then cut into strips using wire EDM and the strips to be effectively given reductions in thickness of 20, 30 & 40% by cold rolling. The shape memory effect (SME), hardness, and super elasticity to be measured for the different conditions. SME effect is intended to be Measured based on the ASTM standards and "Determination of Transformation Temperature of Nickel-Titanium Shape Memory Alloys to be accomplished by Bend and Free Recovery". The experiment to be designed such that both the cold rolled and the as-received samples would be subjected to bending strain values of 2.5, 5 and 10% using the three point bending test. According to the equation $\varepsilon=T/D$, The choice of the sample thickness (T) and mandrels diameters (D) to be made according to the desired bending strain values (ε). According to the ASTM standard, alloys that are super elastic at room temperature should be tested for martensitic transformation in an alcohol bath and has to be loaded at critical temperature to test for the effect of cold working on the ternary alloy system. After bending, the samples to be removed from the fixture and the spring back angle to be measured, θ_{sp}, without removing the samples from the cold bath. $\theta_{sp\ is}$ the angle between the two ends of the sample while still inside the cold alcohol bath. The samples to be removed from the alcohol bath into the atmosphere, where the samples should recover back to the austenite phase, and the final angle reached after recovery to be measured, θ_f. The shape memory recovery (SMR) to be then measured with appropriate calculations. As-cast and cold rolled samples to be tested for hardness with 12-25 indents performed on each, fatigue, wear (abrasive and adhesive wear on pin on disc type of wear testing machine), and super elasticity. (In order to measure super elasticity Polynomial regression to be used to find equations that fit both the loading and unloading curve of each indent since these curves are supposed to a polynomial relation. The equations that are obtained to be then integrated and the ratio of the area under unloading curve to the area under the loading curve to be effectively computed).

III. EXPERIMENTAL WORK

Choosing the composition of the alloy with varying Iron contents

Table 3.1: Selected alloy compositions (atomic %) for experimental work

Alloy	Ti (At %)	Ni (At %)	Fe (At %)	Total (%)
NiTi	50	50	0	100
NiTiFe	50	46	4	100
NiTiFe	50	42	8	100

Table 3.2 Atomic mass of the raw material

Material	Atomic Mass
Ti	47.88
Ni	69.00
Fe	55.84

ISSN 2277 – 5528
Impact Factor- 4.015

To weigh out the materials conversion from at (%) to wt (%) is done by using following relation

$$Wt\%A = \frac{atom\%A * at\ wt\ A}{(Atom\%\ A * wt\ A) + (Atom\%\ B * at\ wt\ B) + (Atom\%vC * at\ wt\ C)} \quad (1)$$

Table 3.3: Alloy composition wt (%) selected for experimental work

Alloy	Ti(At%)	Ni(At%)	Fe(At%)	Total(%)
NiTi	44.932	55.070	0	100.000
NiTiFe	45.000	50.850	4.150	100.000
NiTiFe	45.070	47.020	8.008	100.000

Table 3.4: 10g composition selected for experimental work

Alloy	Ti(gms)	Ni(gms)	Fe(gms)	Total(gms)
NiTi	4.4932	5.507	0	10
NiTiFe	4.500	5.085	0.415	10
NiTiFe	4.507	4.702	0.800	10

The metals are weighed accurately to the above values shown in Table 3.3, 3.4 separately and taken for melting in vacuum arc melting furnace. This is done by striking an electrical arc between a tungsten electrode and the raw material on a water-cooled copper strike plate. Melting is done in Argon, and the mould itself is water cooled copper, so no carbon is introduced during melting. The experimental SMA ingots were prepared through no consumable vacuum arc melting process by using a water-cooled copper hearth in argon atmosphere. Ti (purity 99.9 wt. %), Ni (purity 99.9 wt. %) and Fe (purity 99.9 wt. %), were mixed together and were repeatedly melted for four times for homogenization. The nominal composition of the as-prepared alloys is $Ti_{50}Ni_{50}$, $Ti_{50}Ni_{47}Fe_3$, $Ti_{50}Ni_{44}Fe_6$, Ti_{50}-$Ni_{41}Fe_9$, in terms of at. %. Then the ingots were sealed in vacuum quartz capsules and underwent homogenization at 850 °C for 24 h followed by quenching in water with the seal unbroken. Homogenized alloys were spark-cut in different gauge dimensions for measurements. The phase transformation was investigated on an electrical resistance (E-R) apparatus with a heating/cooling rate of 1 K/min. Optical microstructure were determined on an Olympus metallographic optical microscope.

IV. RESULT & DISCUSSION

Microstructure of Ni_{50} $Ti_{50-x}Fe_x$

Optical microscopy

Fig.4.1.1 shows the optical micrographs of $Ti_{50}Ni_{50}$-x Fe_x(x=0, 4, 8) alloys. It is noted that the as-homogenized alloys are characterized by large grains (100-500 μm) and uniform composition. In comparison with the clean morphology of $Ti_{50}Ni_{46}Fe_4$, many small black spherical precipitates are observed inside the grains as well as along the grain boundaries in the Fe containing alloys (see Fig.4.1.1 (b)-Fig.4.1.1 (e)). However, no obviously contrasting morphology is discovered in the low-resolution images. Further microstructural details can be identified by using back-scattering electron microscopy. Both heat treated (HT) and without heat treated (WHT) images shown below.

ISSN 2277 – 5528
Impact Factor- 4.015

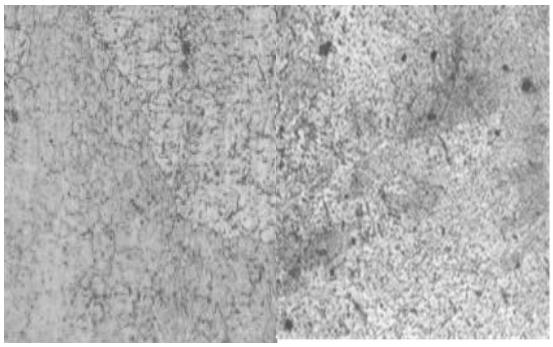

(a)NiTi as-cast condition *(b) NiTi heat treated (300 °c)*

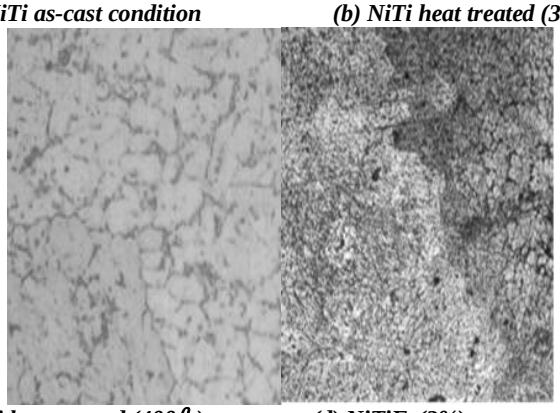

(c) NiTi heat treated (400 °c) *(d) NiTiFe(3%) as cast condition*

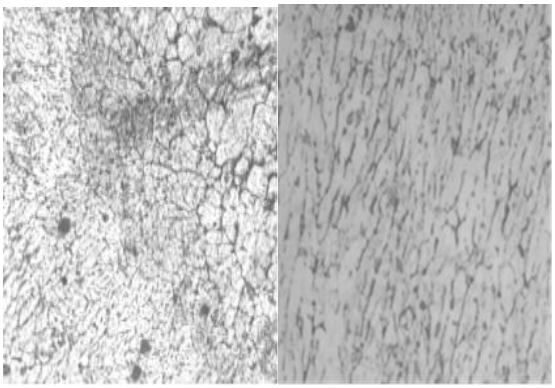

(e) NiTiFe(3%) heat treated (300 °c) *(f) NiTiFe(3%) heat treated (400 °c)*

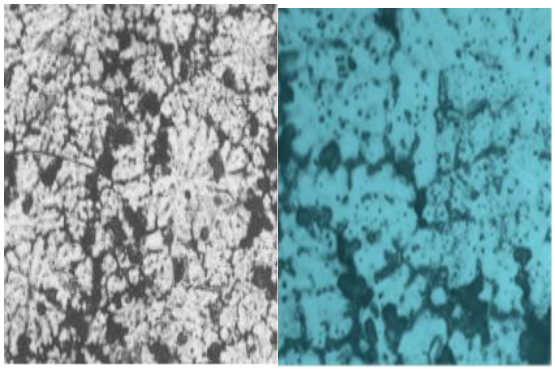

(g) NiTiFe(9%) as cast condition *(h) NiTiFe(9%) heat treated (300 °c)*

ISSN 2277 – 5528
Impact Factor- 4.015

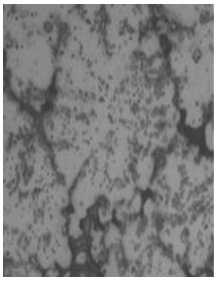

(i) NiTiFe(9%) heat treated (400 ^{0}c)
Fig 4.1.1: Optical images of $Ti_{50}Ni_{48-x}Fe_x$ SMAs.

Differential Scanning Calorimetry

First DSC runs were attempted from room temperature and up on casts without any luck. The cast samples are heavily cored, with residual stresses from rapid solidification and with the possibility of higher Ni in Nitinols failed to reveal any reaction during heating up from ambient or during cooling. Hence the tests were performed on a low temperature setup. The graphs below show the transformation temperature ranges for the different compositions of Nitinol in both as-cast and heat-treated conditions

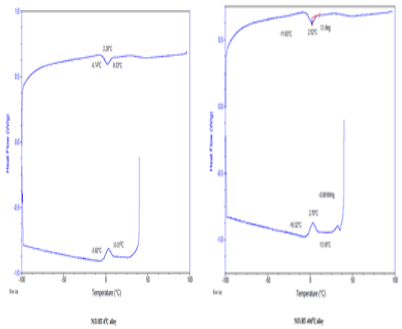

Fig. 4.2(a) DSC curve for as-cast NiTi alloy Fig. 4.2(b) DSC curve for NiTi-HT 400 ^{o}C alloy

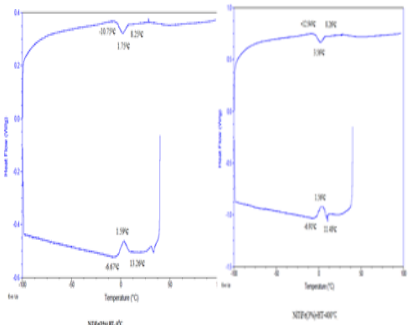

Fig. 4.2(c) DSC curve for as-cast NiTiFe(4%) alloy Fig. 4.2(d) DSC curve for NiTiFe (4%)-HT 400^{o}C alloy

ISSN 2277 – 5528
Impact Factor- 4.015

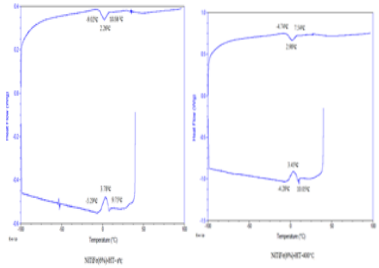

Fig. 4.2(e) DSC curve for as-cast NiTiFe(8%) alloy Fig. 4.2(f) DSC curve for NiTiFe (8%)-HT 400^{o}C alloy

X-Ray Diffraction

The figures below demonstrate the X-ray diffraction curves for both the as-cast and the heat-treated Nitinol alloys

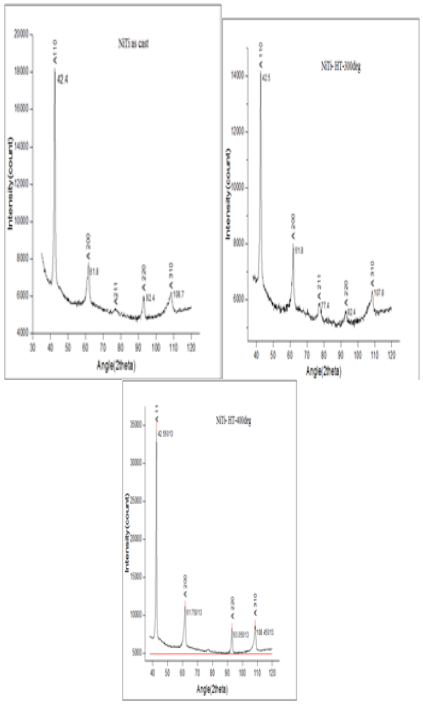

Fig. 4.31(a)(b)(c) XRD graphs of NiTi specimens

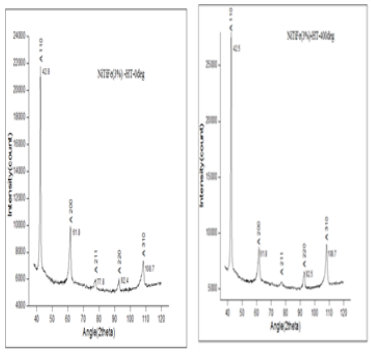

ISSN 2277 – 5528
Impact Factor- 4.015

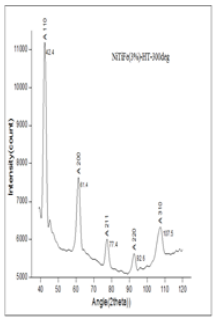

Fig. 4.32(a)(b)(c) XRD graphs of NiTiFe(4%) specimens

Hardness

Hardness test is performed on vicker's hardness tester equipment. micro-hardness testing was done on the specimens. the test surfaces of the specimens are well polished. load of 2kg was applied to test the specimens. during the test a square based 136^0 shaped diamond indentor was used in testing. the rhombus is formed on the specimen surface when it has hit by the diamond indentor. the diagonals of these rhombus is measured and hardness is measured using the formula

$$Vicker's\ Hardness\ HV = \frac{1.854 * f}{d^2} \qquad (2)$$

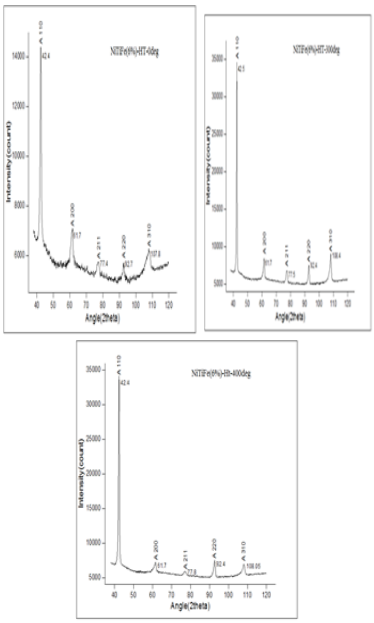

Fig. 4.33(a)(b)(c) XRD graphs of NiTiFe(8%) specimens

where 'F' is the load applied in kg and 'D' is the mean of lenghts of the diagonals of square indentation.

And the hardness value got for different composition is shown in table 4.4.1 and Hardness plot against different specimen composition for Before heat treatment and After heat treated specimens is shown in fig 4.4.1.

ISSN 2277 – 5528
Impact Factor- 4.015

Table 4.4.1: Hardness Results For Before Heat Treatment and After Heat Treatment

SPECIMENS	BEFORE HEAT TREATMENT	AFTER HEAT TREATMENT
Ni-50% , Ti-50% , Fe 0%	310.3	318.3
Ni-46% , Ti-50% , Fe 4%	286.7	324.7
Ni-42% , Ti-50% , Fe 8%	345.5	296.8

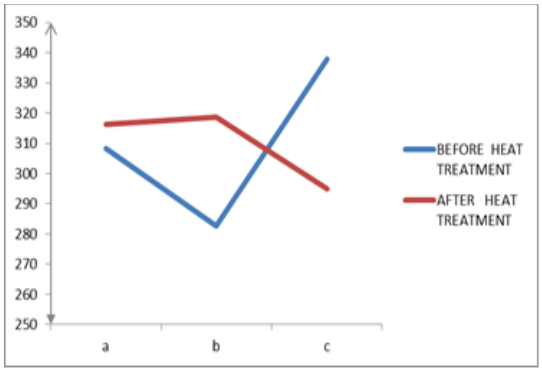

a:- Ni(50%) Ti(50%) Fe(0%), b:- Ni(46%) Ti(50%) Fe(4%) c:- Ni(41%) Ti(50%) Fe(8%)

Fig 4.4.1: Hardness plot against different specimen composition Before heat treatment and After heat treatment

V. CONCLUSION

After successful completion of the experimentation on wear and corresponding hardness characteristics of specimen,the following conclusion can be drawn. The hardness of the ternary alloy is found to increase for iron content varying from 4 to 8% whereas it seems to be decreasing for less than 4%.The experimentation conducted on wear characteristics have given results in which the wear iNiTially increases with increase in iron percentage but after 4% it is going to decrease with increased addition of iron.The comparitive evaluation made on ternary alloy system before and after heat treatment have shown that the hardness increases for NiTi alloy and NiTiFe alloy with fe(iron) in the alloying percentage of 4% whereas it decreases for 8%. In the proposed work, the ternary alloy iron is added for martensite suppression which is basically very much necessary for orthodentic implantation. Hence forth we have carried out experimentation to predict the affect of iron on NiTi binary alloy system .It is found from optical microscopy that the grain size of NiTi atoms are ranging in between 7.5 to 8μm^2 and the iron atoms are found to be distributed all around the grain boundaries.It is seen from the above micrographs taken at 100x, 200x and 500x that the NiTiFe reveal fine structures showing various precipitates that are black streaks running through the structure in the NiTi matrix. These fine precipitates are formed along with the NiTi and represent the Fe dispersed along the grain boundaries of NiTi and NiTi forms a strong intermetallic bond with distinct grain peripheries being visible in the microstructure. It is seen from the above micrographs that the grains in heat treated samples have undergone coring (micro-segregation) with fine dendritic growth of NiTi phase with the interdendritic filling of eutectics mostly TiFe intermetallic bonds being formed along the grain boundary of Ni atoms. Also it is clearly visible that in $NiTiFe_{x=8}$ samples there is growth or coarsening of the cast structure and it is observed that the grains have begun appear with the strong contrast of the cast structure receding. The internal stresses in the sample may start to decrease because of growth of micro constituents. Further in the heat-treated samples the grains of NiTi are seen clearly as the cast dendrites have totally disappeared. The 40-60 micron sized grains of NiTi reveal the presence of very fine precipitates of Fe of the range of 7.5-8 microns around the periphery of grains due to aging along with some coarse ones that originated during solidification of molten metal.

REFERENCES

1. *Otsuka K, Ren X. "Recent Developments in the Research of Shape Memory Alloys". Intermetallic 1999; 7(5): 511-528.*
2. *Jani JM, Leary M, Subic A, Gibson MA. A review of shape memory alloy research, applications and opportunities. Materials & Design. 2014 Apr 30; 56:1078-113.*
3. *Liu Y, Genzer J, Dickey MD. "2D or not 2D": Shape-programming polymer sheets. Progress in Polymer Science. 2016 Jan 31; 52:79-106.*
4. *Karaca HE, Saghaian SM, Ded G, Tobe H, Basaran B, Maier HJ, Noebe RD, Chumlyakov YI. Effects of nanoprecipitation on the shape memory and material properties of a Ni-rich NiTiHf high temperature shape memory alloy. Acta Materialia. 2013 Nov 30; 61(19):7422-31.*
5. *Kaynak Y, Karaca HE, Noebe RD, Jawahir IS. Tool-wear analysis in cryogenic machining of NiTi shape memory alloys: A comparison of tool-wear performance with dry and MQL machining. Wear. 2013 Aug 30; 306(1):51-63.*
6. *Rahim M, Frenzel J, Frotscher M, Pfetzing-Micklich J, Steegmüller R, Wohlschlögel M, Mughrabi H, Eggeler G. Impurity levels and fatigue lives of pseudoelastic NiTi shape memory alloys. Acta Materialia. 2013 Jun 30; 61(10):3667-86.*
7. *Fadlallah SA, El-Bagoury N, El-Rab SM, Ahmed RA, El-Ousamii G. An overview of NiTi shape memory alloy: corrosion resistance and antibacterial inhibition for dental application. Journal of Alloys and Compounds. 2014 Jan 15; 583:455-64.*
8. *Saghaian, S. M., et al. "Effects of aging on the shape memory behavior of Ni-rich Ni 50.3 Ti 29.7 Hf 20 single crystals." Acta Materialia 87 (2015): 128-141.*
9. *Niendorf T, Krooß P, Somsen C, Eggeler G, Chumlyakov YI, Maier HJ. Martensite aging–Avenue to new high temperature shape memory alloys. Acta Materialia. 2015 May 1; 89:298-304.*
10. *Van Humbeeck J. Non-medical applications of shape memory alloys. Materials Science and Engineering: A. 1999 Dec 15; 273:134-48.*
11. *Jani JM, Leary M, Subic A, Gibson MA. A review of shape memory alloy research, applications and opportunities. Materials & Design. 2014 Apr 30; 56:1078-113.*
12. *Sun L, Huang WM, Ding Z, Zhao Y, Wang CC, Purnawali H, Tang C. Stimulus-responsive shape memory materials: a review. Materials & Design. 2012 Jan 31; 33:577-640.*
13. *Ogawa Y, Ando D, Sutou Y, Koike J. A lightweight shape-memory magnesium alloy. Science. 2016 Jul 22; 353(6297):368-70.*
14. *Reedlunn B, Churchill CB, Nelson EE, Shaw JA, Daly SH. Tension, compression, and bending of superelastic shape memory alloy tubes. Journal of the Mechanics and Physics of Solids. 2014 Feb 28; 63:506-37.*
15. *Yu C, Kang G, Kan Q, Song D. A micromechanical constitutive model based on crystal plasticity for thermo-mechanical cyclic deformation of NiTi shape memory alloys. International Journal of Plasticity. 2013 May 31; 44:161-91.*
16. *Pogrebnjak AD, Bratushka SN, Beresnev VM, Levintant-Zayonts N. Shape memory effect and superelasticity of titanium nickelide alloys implanted with high ion doses. Russian Chemical Reviews. 2013; 82(12):1135.*
17. *Liu Y, Kohl M, Okutsu K, Miyazaki S. A TiNiPd thin film microvalve for high temperature applications. Materials Science and Engineering: A. 2004 Jul 25; 378(1):205-9.*
18. *Mohri M, NiliAhmadabadi M, Ivanisenko J. On the Super-Elastic and Phase Transformation of a Novel Ni-Rich/NiTiCu Bi-Layer Thin Film. Advanced Engineering Materials. 2015 Jun 1; 17(6):856-65.*
19. *Buenconsejo PJ, Ludwig A. Composition–structure–function diagrams of Ti–Ni–Au thin film shape memory alloys. ACS combinatorial science. 2014 Nov 14; 16(12):678-85.*
20. *Dwevedi S, Dahilya MK, Tiwari B. Structural, Magnetic, and Transport Properties of NiTiIr Shape Memory Alloy. Journal of Superconductivity and Novel Magnetism. 2016:1-4.*
21. *Xu H, Jiang C, Gong S, Feng G. Martensitic transformation of the Ti 50 Ni 48 Fe 2 alloy deformed at different temperatures. Materials Science and Engineering: A. 2000 Apr 15; 281(1):234-8.*
22. *Ahmed RA. Electrochemical properties of Ni47Ti49Co4 shape memory alloy in artificial urine for urological implant. Industrial & Engineering Chemistry Research. 2015 Aug 20; 54(34):8397-404.*
23. *Chen B, Liu FS. Phase transformation behaviour and mechanical properties of Ti50Ni49− x Fe1Co x shape memory alloys. Rare Metals. 2013 Jun 1; 32(3):225-7.*

ISSN 2277 – 5528
Impact Factor- 4.015

24. *Yuan XB, Chen B, Liu FS, Xu Q, Ma W. Transformation behaviours and super elasticity of Ti50Ni48Fe2 shape memory alloy subjected to cold-rolling and subsequent annealing. Rare Metals. 2014 Dec 1; 33(6):652-6.*
25. *Li Y, Feng X, Mi X, Yin X, Kang X. Microstructure and Mechanical Properties of TiNiFe Shape Memory Alloys with Different Compositions. InMaterials Science Forum 2016 Feb 2 (Vol. 849).*
26. *Zheng YF, Zhao LC. NiTi alloys applied in the medical field.*
27. *Hsieh SF, Wu SK. A study on ternary Ti-rich TiNiZr shape memory alloys. Materials characterization. 1998 Oct 31;41(4):151-62.*
28. *Frenzel J, Pfetzing J, Neuking K, et al. "On The Influence Of Thermo mechanical Treatments On The Microstructure And Phase Transformation Behaviour Of Ni- Ti-Fe Shape Memory Alloys". Materials Science and Engineering a 2008; 482-484(4): 635-638.*
29. *Xu Z Y. "Shape Memory Materials". Shanghai: Shanghai Jiaotong UNiversity Press, 2000. [in Chinese]*
30. *Hwang C M, Meichle M, Salamon M B, et al. "Transformation Behaviors Of A Ti50Ni47Fe3 Alloy Subsequent Premartensitic Behavior And The Commensurate Phase". Philosophical Magazine a 1983; 47(9): 31-36.*